GREEN SYNTHESIS AND CHARACTERIZATION OF SILVER NANOPARTICLES USING ARTOCARPUS HETEROPHYLLUS LEAVES EXTRACT

Mindi Ramakrishna[1], Nalluri Chitti Babu[2]*, Salla Asiri Naidu[3], Dakshayini Goonapu[4]

Article History: **Received: 22.10.2022** **Revised: 30.10.2022** **Accepted: 05.11.2022.**

Abstract: In the present study, an environmentally benign process of synthesis of the silver nanoparticles (Ag NPs) using Artocarpus Heterophyllus (Jack Fruit Leaves) as both stabilizing and reducing agents. The nanoparticles formation was observed by color change from pale yellow to dark brown. The effect concentration ratio of leaves extract intake and of silver nitrate solution on synthesis of Ag NPs was studied. The synthesized nanoparticles are characterized by XRD, SEM and FTIR techniques to analyze size, morphology and functional groups. The formation of silver nanoparticles was confirmed from UV spectroscopic technique. The crystallographic structure of synthesized Ag NPs was recognized using powder XRD technique. The presences of organic and inorganic compounds in synthesized nanoparticles were identified using FTIR analysis. The average size of synthesized nanoparticles was estimated using XRD patterns and SEM analysis.

Keywords: Artocarpus Heterophyllus, Silver Nitrate Solution, Silver Nanoparticles, Characterization Techniques.

[1]Ph.D Scholar, Department of Chemical Engineering, Andhra University College of Engineering, Visakhapatnam, Andhra Pradesh-530003, India.
[2*]Professor, Department of Chemical Engineering, Andhra University College of Engineering, Visakhapatnam, Andhra Pradesh-530003, India.
[3]Assistant Professor, Department of Chemistry, Rajiv Gandhi University of Knowledge Technologies, Srikakulam, Andhra Pradesh-532402, India.
[1,4]Department of Chemical Engineering, Rajiv Gandhi University of Knowledge Technologies, Nuzvid, Andhra Pradesh-521202, India.

***Corresponding Author:** Nalluri Chitti Babu
*Professor, Department of Chemical Engineering, Andhra University College of Engineering, Visakhapatnam, Andhra Pradesh-530003, India.
Email: nallurichitti@rediffmail.com, krishna019@rguktn.ac.in

DOI: 10.53555/ecb/2022.11.11.82

Introduction:

Nowadays nanotechnology plays a pivotal role in advancement of science and technology. Nanomaterials have a size of 1 to 100 nanometers.[1,2] At this size nanomaterials possess some unique properties like large surface area and small dimensions which affects the physical, chemical and biological properties.[3,4] So they are having wide range of applications in many fields like medicine,[5,6] dye removal,[7,8] industrial and energy uses.[9-12]

A wide range of nanoparticles have been termed unceremoniously through the years including nanospheres, nanorods, nanochains, nanostars, nanoflowers, nanoreefs, nanowhiskers, nanofibers and nanoboxes.[13-16] Nanoparticles can have different shapes based on their intrinsic crystal habit or their environment around while formation. Inhibiting crystal growth by coating certain faces with additives, forming emulsion droplets and micelles when preparing precursors, and shaping pores within solid materials are examples of these factors.[17] In some applications, nanoparticles may need specific shapes, as well as specific sizes or sizes ranges. Despite their amorphous nature, amorphous particles tend to shape up as spheres (owing to their isotropy at a micro structural level). In nanoparticle form, a material's properties differ significantly from its bulk properties even when divided into micrometer-sized segments.[18-20]

Additionally, nanoparticles can be synthesized by physical, chemical, and biological methods, but these are less preferred by reason of their high maintenance costs, toxic reducing agents, and long degradation times. Phytochemicals present in plant leaves have anti-oxidant or reducing properties that enable metal nanoparticles to be synthesized.[21] Ag NPs are among the most widely used nanomaterials due to their antimicrobial, electrical, and optical properties.[22,23] Silver nanoparticles are nanoparticles of silver of between 1 nm and 100 nm in size. Commonly used silver nanoparticles are spherical, but diamond, octagonal, and thin sheets are also common. The large surface area of these molecules allows them to coordinate a large number of ligands. Researchers are examining the properties of Ag NPs that might be useful for human treatments in animal studies, assessing their potential efficacy, toxicity, and cost. In order to synthesize Ag NPs, different physical and chemical methods can be used. It was, however, the high production costs and toxicity problems associated with the above techniques that opened up the door to an efficient, reliable, and environmentally benign green chemistry method. Many studies have been conducted on the green synthesis of Ag NPs using various leaves, such as guava and neem, aloe vera, lemon, hibiscus, tulasi, and so forth, but most have focused on their antibacterial properties.[24-27] Dye removal from green synthesized Ag NPs using various dye molecules, however, is rarely investigated.[28,29]

Materials and Methodology:

i) Materials:

1. Artocarpus Heterophyllus(Jack Fruit) leaves powder
2. Silver Nitrate ($AgNO_3$, Fisher Scientific, 99.8%)
3. Distilled Water
4. Whatman Filter Paper

ii) Methodology:

Artocarpus Heterophyllus leaves were cleaned using distilled water and Sun dried for two days, and the dried leaves powder was prepared from the leaves. 20 grams of Artocarpus Heterophyllus leaves powder was taken into a beaker along with 200 ml of distilled water. The solution mixture is subjected to continuous stirring at 400 rpm and heating at 50ºC respectively using magnetic stirrer for 30 minutes. The obtained solution is filtered using Whatman filter paper and the leaves extract is separated. 100 ml of 6 mM silver nitrate solution is prepared. The prepared 10 to 20 samples containing 2 ml of silver nitrate solution and 10 ml of leaves extract forms a pale yellow colored solution. The samples were stored in a dark chamber for 60 - 120 minutes, observed the color change from pale yellow to dark brown. The formation of Ag NPsis confirmed upon the colour change from pale yellow to dark brown.

Figure-1: Artocarpus Heterophyllus (Jack Fruit) Leaves.

The same process was repeatedly performed for different ratios of leaves powder and distilled water i.e., 1:10, 1:20 for two concentrations of $AgNO_3$ solution i.e 6mM and 10mM. The samples, after observing the color change were centrifuged at 6000 rpm for 30 minutes using centrifuge apparatus. The particles formed were separated using filtration and cleaned twice using distilled water and dried for 10 min at 50ºC to obtain silver nanoparticles powder. The obtained silver nanoparticles powder from all the four cases were further characterized using UV-spectroscopy, XRD, FTIR and SEM analysis.

Results and Discussion:

Characterization of Ag – Nanoparticles

A) UV - Visible Spectroscopy Analysis:

Figure-2 (a), (b), (c) and (d) shows the UV-visible absorption spectrum of silver nanoparticles that were synthesized using jack fruit leaves at two different ratios of leaves powder and distilled water for two different molarities of $AgNO_3$ solution i,e 1:10 - 6mM, 1:10 - 10mM, 1:20 - 6mM, 1:20 - 10mM respectively.

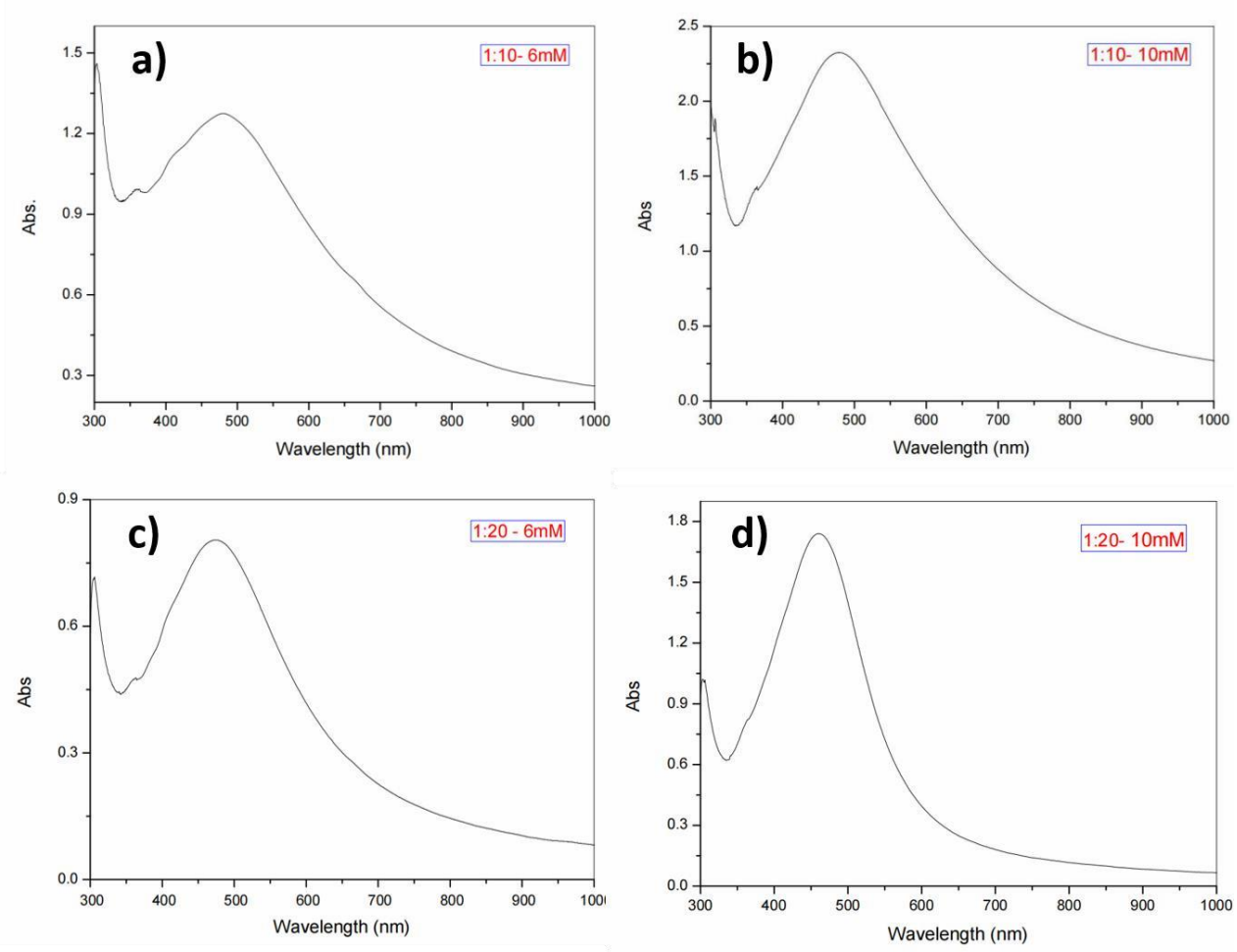

Figure-2: (a), (b), (c), and (d) are UV- visible spectrum of green synthesized silver nanoparticles for four different cases.

The presence of absorbance peak for the four cases are in the range of 450 - 500 nm indicates the formation of silver nanoparticles.[24,30] The absorbance spectra of silver nanoparticles synthesized using jack fruit leaves show an additional peak at around 370 nm, which can be associated to the quadrupolar resonance in besides the primary dipole resonance. The same observations were reported by Garcia et al., with aloe vera leaves extract.[31]

B) X - Ray Diffraction Analysis:

The phase purity and crystalline nature of the Ag nanoparticles was further confirmed from the powder XRD technique. Figure-3(a), (b), (c) and (d) shows the XRD patterns of the green synthesized silver nanoparticles using jack fruit leaves (Artocarpus Heterophyllus) extract.

The observed XRD patterns establish the single-phase nature of the Ag nanoparticles and no impurity peaks were identified.

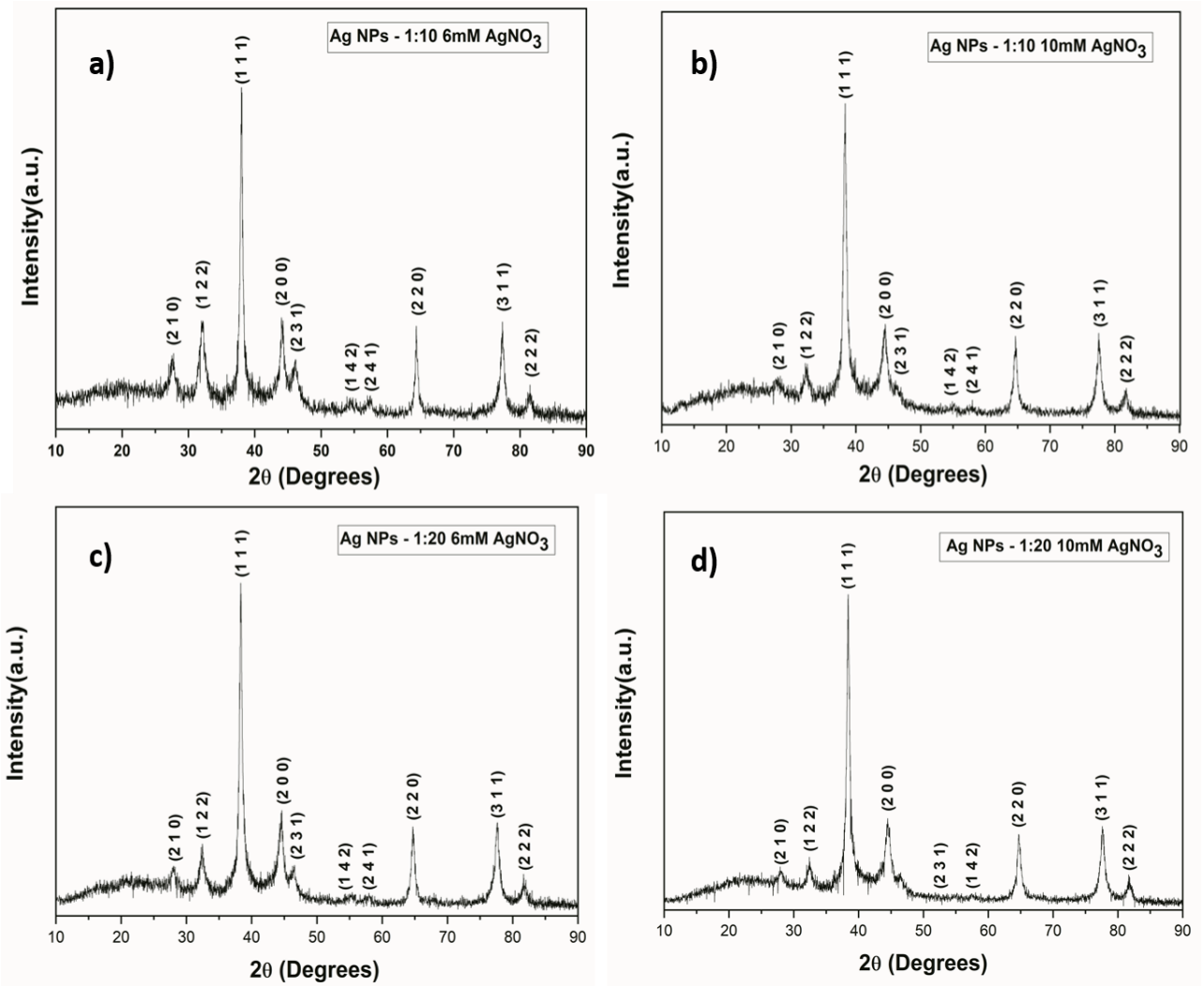

Figure-3: (a), (b), (c) and (d) are X-Ray Diffraction Analysis of green synthesized silver nanoparticles for four different cases mentioned above.

Five peaks at 2θ values of 27.9775, 32.3713, 38.3246, 44.4028, 64.6473, 77.5578 and 81.6357 degrees corresponding to (210), (122), (111), (200), (220), (311) and (222) planes of silver is observed and compared with the standard powder diffraction pattern of Joint Committee on Powder Diffraction Standards (JCPDS # 04–0783).

XRD – Particle Size Calculation:

In the present study, considering the peak at degrees, average particle size has been calculated by using Debye-Scherrer formula.[32,33]

$$D = \frac{0.9\lambda}{\beta Cos\theta}$$

Where 'λ' is the wave length of X-Ray (0.1541862 nm), 'β' is FWHM (Full width at half maximum), 'θ' is the diffraction angle and 'D' is particle diameter size. The calculated particle size details are given in Table: 1(a) – 1(d).

Table-1(a): The grain size of Silver NanoPowder (for the Case: Ag NPs – 1:10 6mM $AgNO_3$).

The Intense Peak Position '2θ' (Degrees)	The Value of 'θ' in (Radians)	hkl	FWHM of Intense Peak 'β' (Degrees)	FWHM of Intense Peak 'β' (Radians)	Crystallite Size of Ag NPs 'D' (nm)	Average Crystallite Size of Ag NPs (nm)
27.59	0.24	(2 1 0)	1.11	0.02	7.71	**11.35**
32.10	0.28	(1 2 2)	1.16	0.02	7.46	
37.99	0.33	(1 1 1)	0.48	0.01	18.31	
44.11	0.38	(2 0 0)	1.18	0.02	7.57	
64.39	0.56	(2 2 0)	0.62	0.01	15.75	
77.32	0.67	(3 1 1)	0.97	0.02	10.98	
81.44	0.71	(2 2 2)	0.94	0.02	11.67	

Table-1(b): The grain size of Silver Nano Powder (for the Case: Ag NPs – 1:10 10mM $AgNO_3$).

The Intense Peak Position '2θ' (Degrees)	The Value of 'θ' in (Radians)	hkl	FWHM of Intense Peak 'β' (Degrees)	FWHM of Intense Peak 'β' (Radians)	Crystallite Size of Ag NPs 'D' (nm)	Average Crystallite Size of Ag NPs (nm)
27.9775	0.2441	(2 1 0)	0.8777	0.0153	9.74	
32.3713	0.2825	(1 2 2)	1.0189	0.0178	8.48	
38.3246	0.3344	(1 1 1)	0.7773	0.0136	11.30	
44.4028	0.3875	(2 0 0)	1.9892	0.0347	4.51	**10.10**
64.6473	0.5642	(2 2 0)	0.7986	0.0139	12.29	
77.5578	0.6768	(3 1 1)	0.9340	0.0163	11.39	
81.6357	0.7124	(2 2 2)	0.8463	0.0148	12.96	

Table-1(c): The grain size of Silver Nano Powder (for the Case: Ag NPs – 1:20 6mM $AgNO_3$).

The Intense Peak Position '2θ' (Degrees)	The Value of 'θ' in (Radians)	hkl	FWHM of Intense Peak 'β' (Degrees)	FWHM of Intense Peak 'β' (Radians)	Crystallite Size of Ag NPs 'D' (nm)	Average Crystallite Size of Ag NPs (nm)
27.98	0.24	(2 1 0)	0.78	0.01	11.02	
32.41	0.28	(1 2 2)	0.92	0.02	9.44	
38.34	0.33	(1 1 1)	0.68	0.01	12.89	
44.45	0.39	(2 0 0)	1.31	0.02	6.83	**10.33**
46.38	0.40	(2 2 0)	1.08	0.02	8.36	
64.73	0.56	(3 1 1)	0.76	0.01	13.00	
77.61	0.68	(2 2 2)	0.99	0.02	10.80	

Table-1(d): The grain size of Silver Nano Powder (for the Case: Ag NPs – 1:20 10mM $AgNO_3$).

The Intense Peak Position '2θ' (Degrees)	The Value of 'θ' in (Radians)	hkl	FWHM of Intense Peak 'β' (Degrees)	FWHM of Intense Peak 'β' (Radians)	Crystallite Size of Ag NPs 'D' (nm)	Average Crystallite Size of Ag NPs (nm)
28.0200	0.2445	(2 1 0)	0.7083	0.0124	12.08	
32.4374	0.2831	(1 2 2)	0.7527	0.0131	11.48	
38.3978	0.3351	(1 1 1)	0.7185	0.0125	12.23	
44.4996	0.3883	(2 0 0)	1.9722	0.0344	4.55	**10.60**
64.7579	0.5651	(2 2 0)	0.8392	0.0146	11.71	
77.6395	0.6775	(3 1 1)	1.0627	0.0185	10.02	
81.7414	0.7133	(2 2 2)	0.9034	0.0158	12.16	

C) Particle size analysis using SEM(Scanning Electron Microscopy) analysis:

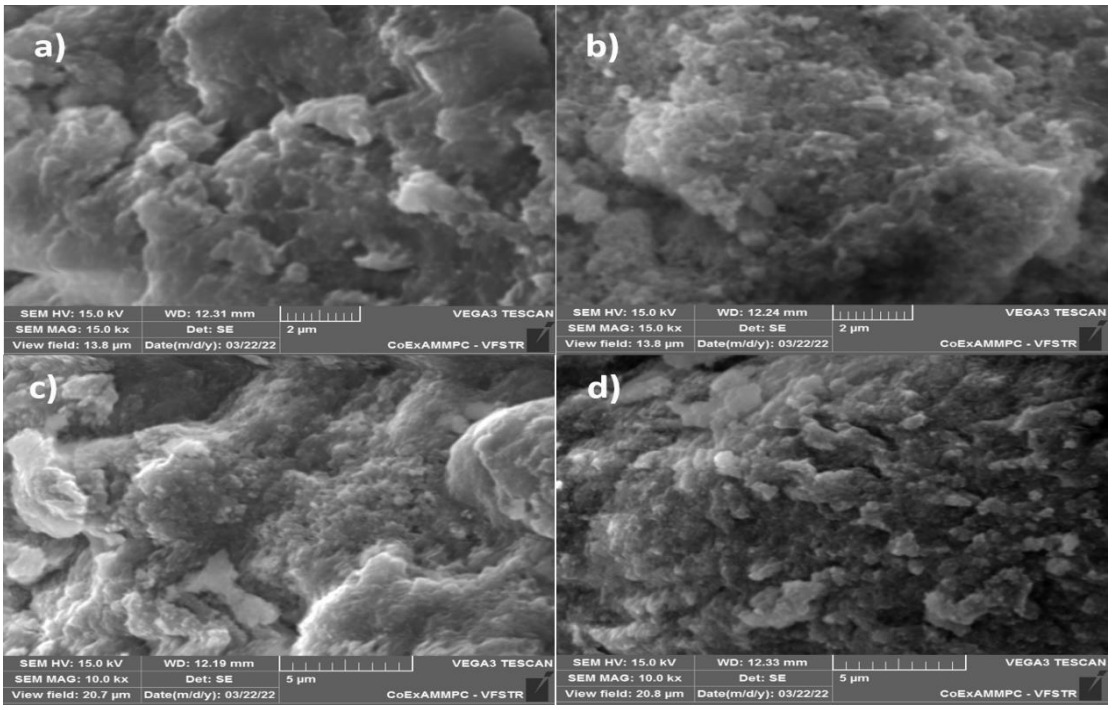

Figure-4: (a), (b), (c) and (d) are SEM images of green synthesized silver nanoparticles for four different cases.

The physical structure of Ag-NPs as shown in the Figure-4 (a), (b), (c) and (d), the Ag NPs surface was irregular and rough. It is quite difficult to confirm the particle size from the recorded SEM micrograms because of the highly agglomerated Ag-NPs. The grain sizes of the samples estimated from the SEM picture is larger than that obtained from XRD data. This means that, the SEM picture indicates the size of polycrystalline particles. Generally, on the nanometer scale, metals (most of them are FCC) tend to nucleate and grow into twinned and multiply twinned particles (MTPs) with their surfaces bounded by the lowest-energy {111} facets. The observation of some larger nanoparticles may be attributed to the fact that Ag nanoparticles have the tendency to agglomerate due to their high surface energy and high surface tension of the ultrafine nanoparticles. The fine particle size results in a large surface area that in turn, enhances the nanoparticles catalytic activity. The SEM images were blurred as the instrument present at the institute was unable to take images of particles below 100nm. The aggregation of Ag particles may be attributed to the smaller ones, because of the SEM measurements.

D) FTIR analysis:

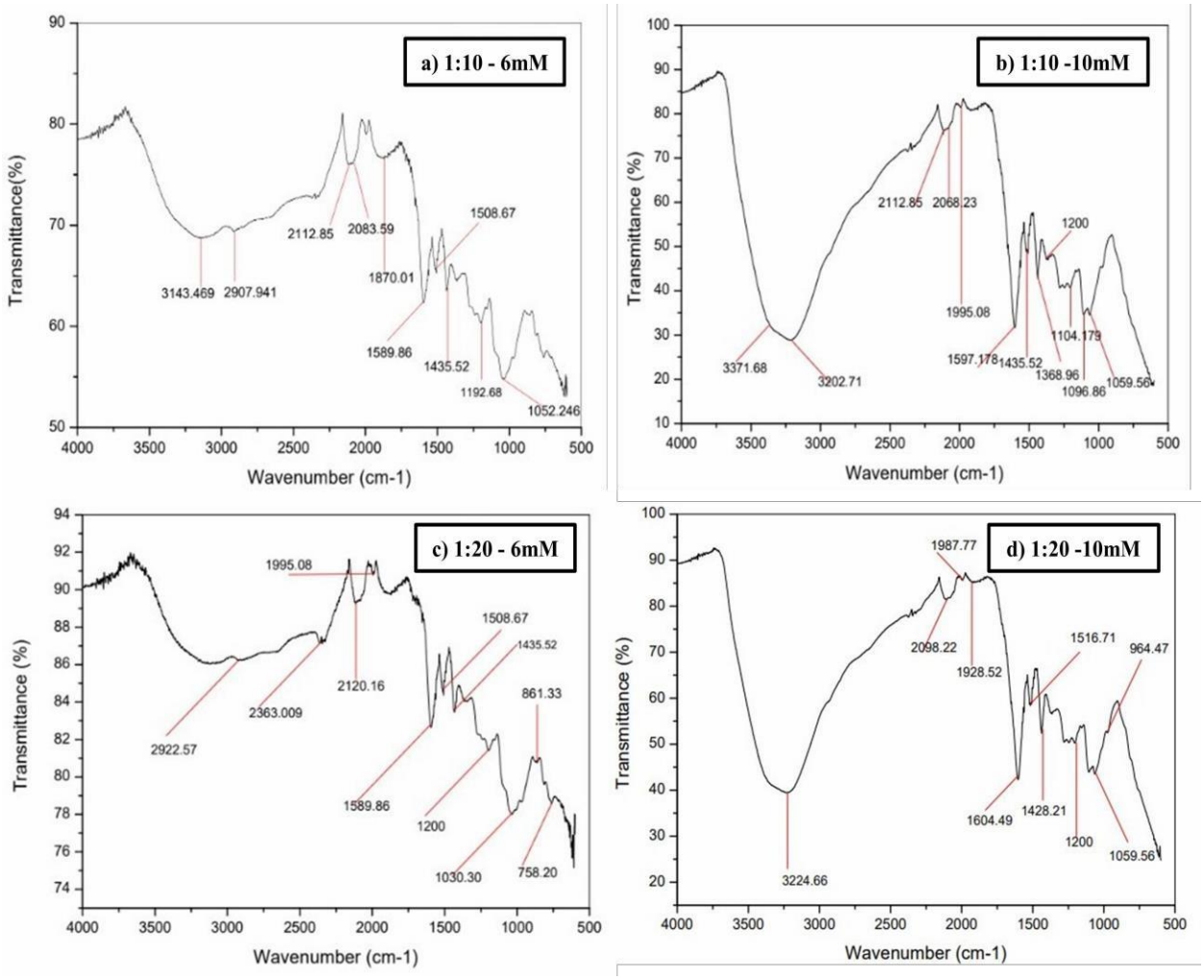

Figure-5: (a), (b), (c), and (d) shows the FTIR spectra of synthesized silver nanoparticles for four different cases i.e 1:10 - 6mM, 1:10 - 10mM, 1:20 - 6mM, 1:20 - 10mM respectively

With the help of FTIR measurements one can get the information around the local molecular environment of the organic molecules on the nanoparticles surface. These measurements were executed to detect the probable biomolecules which are accountable for capping and efficient stabilization of the metal nanoparticles synthesized by jack fruit leaves extract. Figure-5 (a)-(d) shows the FTIR spectra of Ag NPs synthesized using leaf extract of different concentrations. From figure-5(a), Broad band around 3200 cm^{-1}corresponding to the stretching modes of N-H/O-H groups. The peaks observed between 3100 – 3000 cm^{-1} can be attributed to

C≡C stretching modes in alkynes. The peak observed at 1589.86 cm^{-1} can be ascribed to C=C, C=N, C=O. The peak with an approximate maximum around 1435.52 cm^{-1} is due to symmetric binding of CH_3. At 1192 cm^{-1}(asymmetry bridge bond C-O-C stretching vibration), peak at 1059 cm^{-1} can be –OH distortion vibration. The peaks between the 1000 – 1300 cm^{-1} are assigned to esters.

From figure-5(b), Broad band around 3300 cm^{-1} corresponding to hydrogen bonded phenols and alcohols or bonded hydroxyl group. A sharp peak at 1597 cm^{-1} can be $C=C$, $C=N$, $C=O$.The peak at 1435 cm^{-1} is due to symmetric binding of CH_3.The peaks between 1096 – 1059 cm^{-1} can be -OH distortion vibration.

From figure-5(c)**,** Broad band around 3000 cm^{-1}corresponding to hydrogen bonded phenols and alcohols or bonded hydroxyl group. The peak at 1435 cm^{-1} is due to symmetric binding of CH_3. The peak at 1589 cm^{-1}can be assigned to C = O. The peak at 1250 cm^{-1} can be assigned to C-N, C-O.

From figure-5(d), Broad band around 3200 cm^{-1}corresponding to hydrogen bonded phenols and alcohols or bonded hydroxyl group. The peak at 1604 cm^{-1} can be assigned to C = O. The peak at 1428 cm^{-1} is due to symmetric binding of CH_3. The peak at 1250 cm^{-1} can be assigned to C-N, C-O. The peak at 1059 cm^{-1} can be -OH distortion vibration.[34,35]

Conclusion:

Silver nanoparticles were successfully synthesized by using Artocarpus heterophyllus extract and silver nitrate aqueous solution. The presence of phytochemicals in Artocarpus heterophyllus was responsible for the reduction of Ag^+ into Ag and it was confirmed with UV-Visible spectra. The crystalline nature of Ag NPs was evident from sharp peaks obtained from the X-ray diffraction. The functional groups present in the synthesized nanoparticles were identified using FTIR analysis. Further the synthesized silver nanoparticles are subjected to SEM analysis. The average crystallite size of Ag NPs was identified in the range of 10 to 11nm determined from XRD patterns. This echo friendly synthesis method of silver nanoparticles may provide a quick, cheap and suitable alternative method.

References

1. Torres-Torres, C; López-Suárez, A; Can Uc, B; Rangel-Rojo, R; Tamayo-Rivera, L; Oliver, A (24 July 2015). "Collective Optical Kerr effect exhibited by an integrated configuration of silicon quantum dots and gold nanoparticles embedded in ion implanted silica". Nanotechnology. 26 (29):295701.
2. Bleeker E A J, Cassee F R, Geertsma R E, et al. Interpretation and implications of the European Commission's definition on nanomaterials; Letter report 601358001. Bilthoven, Netherlands: RIVM; 2012.
3. S.P. Dubey, M. Lahtinen, M. Sillanpää, Green synthesis and characterizations of silver and gold nanoparticles using leaf extract of Rosa rugosa, Colloids Surf.A, 364(2010), pp.34-41.
4. A.D.Dwivedi, K.Gopal, Biosynthesis of silver and gold nanoparticles using Chenopodium album leaf extract, Colloids Surf., A, 369 (2010), pp. 27-33.
5. Donner, A., Trends Mol. Med., 2010, 16, 551-552.
6. Roco, M. C., Curr. Opin. Biotechnol. 2003, 14, 337-346.
7. Perelshtein, I., Applerot, G., Perkas, N., Guibert, G., Mikhailov, S., Gedanken, A., Nanotechnology, 2008, 19, 245705.
8. Wang, R. R., Nasir, A., Nanotechnology in Dermatology, Springer, 2013, 41-49.
9. Daisy Philip, Physics E 42(2010) Green synthesis of gold and silver nano particle using hibiscus roasa sinensis.
10. S. Ashok kumar, S. Ravi, S. Velmurugan, Green synthesis of silver nanoparticles from Gloriosa superba L. leaf extract and their catalytic activity, Spectrochimica Acta PartA: Molecular and Biomolecular Spectroscopy, 115 (2013), pp. 388-392.
11. P. Banerjee, M. Satapathy, A. Mukhopahayay, P. Das, Leaf extract mediated green synthesis of silver nanoparticles from widely available Indian plants: synthesis, characterization, antimicrobial property and toxicity analysis, Bioresources and Bioprocessing, 1 (3) (2014), pp. 1-10.
12. H. Padalia, P. Moteriya, S. Chanda, Green synthesis of silver nanoparticles from marigold flower and its synergistic antimicrobial potential, Arabian Journal of Chemistry (2014).
13. Agam, M. A; Guo, Q (2007). "Electron Beam Modification of Polymer Nanospheres". Journal of Nanoscience and Nanotechnology. 7 (10): 3615–9.

14. Kralj, Slavko; Makovec, Darko (27 Oct 2015). "Magnetic Assembly of Super paramagnetic Iron Oxide Nanoparticle Clusters into Nanochains and Nanobundles". ACS Nano. 9 (10): 9700–7.
15. Choy J.H.; Jang E.S.; Won J.H.; Chung J.H.; Jang D.J. & Kim Y.W. (2004). "Hydrothermal route to ZnO nanocoral reefs and nanofibers". Appl. Phys. Lett. 84 (2): 287.
16. Sun, Y; Xia, Y (2002). "Shape-controlled synthesis of gold and silver nanoparticles". Science. 298 (5601): 2176–9.
17. Murphy C. J. (13 Dec 2002). "MATERIALS SCIENCE: Nanocubes and Nanoboxes". Science. 298 (5601): 2139–2141.
18. Buzea, Cristina; Pacheco, Ivan I.; Robbie, Kevin (December 2007). "Nanomaterials and nanoparticles: Sources and toxicity". Biointerphases. 2 (4): MR17–MR71.
19. ASTM E 2456 06 Standard Terminology Relating to Nanotechnology.
20. Valenti G, Rampazzo R, Bonacchi S, Petrizza L, Marcaccio M, Montalti M, Prodi L, Paolucci F (2016). "Variable Doping Induces Mechanism Swapping in Electro generated Chemiluminescence of Ru(bpy) 32+ Core Shell Silica Nanoparticles". J. Am. Chem. Soc. 138 (49): 15935–15942.
21. Jerry, O. Adeyemi, Ayodeji, O. Oriola, Damian, C. Onwudiwe, and Adebola, O. Oyedeji (2022). "Plant Extracts Mediated Metal-Based Nanoparticles Synthesis and Biological Applications". Biomolecules 12(5), 627.
22. Abbaszadegan A., Ghahramani Y., Gholami A., Hemmateenejad B., Dorostkar S., Nabavizadeh M., Sharghi H. The Effect of Charge at the Surface of Silver Nanoparticles on Antimicrobial Activity against Gram-Positive and Gram-Negative Bacteria: A Preliminary Study. J. Nanomater. 2015; 2015:1–8.
23. Shenashen MA, El-Safty SA, Elshehy EA. Synthesis, Morphological Control, and Properties of Silver Nanoparticles in Potential Applications. Part. Syst. Charact. 2014; 31: 293-316.
24. Jain, S.; Mehata, M. S. Medicinal plant leaf extract and pure flavonoid mediated green synthesis of silver nanoparticles and their enhanced antibacterial property. Sci. Rep. 2017, 7, 15867.
25. Verma, A.; Mehata, M. S.; Controllable synthesis of silver nanoparticles using Neem leaves and their antimicrobial activity. J. Radiat. Res. Appl. Sci. 2016, 9, 109– 115.
26. Shinde, N. M.; Lokhande, A. C.; Lokhande, C. D. A green synthesis method for large area silver thin film containing nanoparticles. J. Photochem. Photobiol., B 2014, 136, 19-25.
27. Tippayawat, P.; Phromviyo, N.; Boueroy, P.; Chompoosor, A. Green synthesis of silver nanoparticles in aloevera plant extract prepared by a hydrothermal method and their synergistic antibacterial activity. Peer J 2016, 4, e2589.
28. Mohan Singh Mehata. Green route synthesis of silver nanoparticles using plants/ginger extracts with enhanced surface plasmon resonance and degradation of textile dye. Mater. Sci. and Engineering: B 2021, 273, 115418.
29. Tamuly, C.; Hazarika, M.; Bordoloi, M.; Das, M. R.; Photocatalytic activity of Ag nanoparticles synthesized by using piper pedicellatum C. DC fruits. Mater. Lett. 2013, 102–103, 1– 4.
30. Roy, P.; Das, B.; Mohanty, A.; Mohapatra, S. Green synthesis of silver nanoparticles using Azadirachta indica leaf extract and its antimicrobial study. Appl. Nano sci. 2017, 7, 843– 850.
31. Garcia, M. A. Surface plasmons in metallic nanoparticles: fundamentals and applications. J. Phys. D: Appl. Phys. 2011, 44, 283001.
32. B.D. Cullity, Elements of X-ray Diffraction, Addison-Wesley Company, USA.
33. Rita John, S. Sasi Florence, Chalcogenide Lett.6, 535 (2009).
34. S. Marimuthu, A. A. Rahuman, G. Rajakumar et al., "Evaluation of green synthesized silver nanoparticles against parasites," parasitology research, vol.108, no.6, pp. 1541–1549, 2011.
35. P. Prakash, P. Gnanaprakasam, R. Emmanuel, S. Arokiyaraj, M. Saravanan Green synthesis of silver nanoparticles from leaf extract of Mimusops elengi, Linn. For enhanced antibacterial activity against multi drug resistant clinical isolates colloids and surfaces B: Biointerfaces, 108 (2013), 255-259.